9-1-2007

Near-Terminator Venus Ionosphere: Evidence for a Dawn/Dusk Asymmetry in the Thermosphere

Jane L. Fox
Wright State University - Main Campus, jane.fox@wright.edu

W. T. Kasprzak

Near-terminator Venus ionosphere: Evidence for a dawn/dusk asymmetry in the thermosphere

J. L. Fox[1] and W. T. Kasprzak[2]

Received 5 February 2007; revised 25 April 2007; accepted 13 June 2007; published 27 September 2007.

[1] Recent models of the near-terminator ionosphere of Venus constructed using neutral density profiles from the VTS3 model of Hedin et al. (1983) have shown that altitudes of the electron density peaks are in agreement with those measured by Pioneer Venus (PV) Orbiter Radio Occultation (ORO) and other radio occultation profiles in the solar zenith angle (SZA) range 60 to 70°, where they are near 140 km (Fox, 2007). The model peaks in the 75–85° range, however, do not decrease in altitude to near 135 km, as do the PV ORO electron density peaks shown in the study of Cravens et al. (1981). We investigate here possible reasons for this decrease. The PV Orbiter Neutral Mass Spectrometer (ONMS) measured densities of CO_2, O, CO, N_2, N, and He for many of the first 600 orbits. We have chosen 10 orbits in the dawn sector and 12 orbits in the dusk sector for which the solar zenith angles at periapsis were in the 75–85° range, and we have examined the ONMS density profiles reported in the PV Unified Abstract Data System. We find that for most of the orbits, the appropriately normalized ONMS measured densities for CO_2 and O are, however, either similar to or larger than those generated from the VTS3 model for the same solar zenith angle and $F_{10.7}$ flux, and the use of these densities in our models would therefore produce a higher, rather than a lower, peak. The VTS3 models are, however, not expected to be accurate in the terminator region because of the small number of spherical harmonics used in the models and the large density changes that are expected near the terminators. We have also investigated a possible dawn/dusk asymmetry in the ionosphere. All the low-altitude PV radio occultation electron density peaks reported in the study of Cravens et al. (1981) in the 70 to 85° range were in the dawn sector at high latitudes. In the VTS3 models, the exospheric temperatures are predicted to be smaller at dawn that at dusk, but the asymmetries are confined to the region above ~165 km. Thus use of the VTS3 model densities and temperatures in the near-terminator dawn sector models cannot produce electron density peaks that are lower in altitude than those in the dusk sector. We suggest that there is a high-latitude asymmetry between the dawn and dusk neutral densities that extends down to within ~20 km above the expected altitude of the electron density peaks, and that produces a significantly asymmetrical ionosphere.

Citation: Fox, J. L., and W. T. Kasprzak (2007), Near-terminator Venus ionosphere: Evidence for a dawn/dusk asymmetry in the thermosphere, *J. Geophys. Res.*, *112*, E09008, doi:10.1029/2007JE002899.

1. Introduction

[2] The Pioneer Venus (PV) Orbiter began in situ measurements in 1978 December, and a suite of instruments provided data about the Venus thermosphere/ionosphere for nearly three diurnal cycles of 225 days each. This was a period of moderately high to high solar activity. Periapsis was maintained below ~200 km in the thermosphere for the first 600 PV orbits from dates 78339 to 80209. (In this method of expressing dates the first two numbers YY specify the last two digits of the year, and the next 3 numbers DDD specify the ordinal day of the year.) The Orbiter Neutral Mass Spectrometer (ONMS) measured number densities of CO_2, O, N_2, CO, N, and He during 75% of the first 600 orbits. Periapsis was between 138 and 150 km for only 12% of the orbits and only about half of these were on the dayside [e.g., *Niemann et al.*, 1980]. The data were obtained for a narrow latitudinal band around 16°N. A global model of neutral densities, the VTS3 model, was developed by *Hedin et al.* [1983]; it was designed to represent empirically the ONMS data, and assumes diffusive equilibrium above ~150 km. The diffusive equilibrium region was connected with the mixed atmosphere down to 100 km using mass density data from the four PV Entry Probes [e.g., *Seiff et al.*, 1980] and from 130 to 180 km using the density data from the PV Bus Neutral Mass Spectrometer (BNMS) [*von Zahn et al.*, 1980]. In construct-

[1]Department of Physics, Wright State University, Dayton, Ohio, USA.
[2]NASA Goddard Space Flight Center, Greenbelt, Maryland, USA.

0148-0227/07/2007JE002899

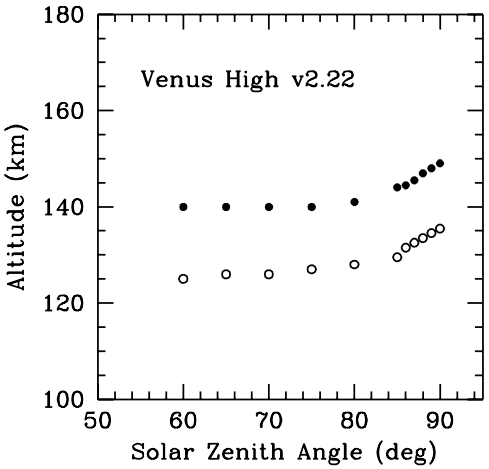

Figure 1. Altitudes of the F_1 and E peaks as a function of SZA for the 60, 65, 70, 75, 80, 85, 86, 87, 88, 89, and 90° models. The filled circles are the F_1 peaks, and the open circles are the E peaks. "v2.22" refers to the Solar 2000 v2.22 solar flux model of *Tobiska* [2004], which was used in constructing the thermosphere/ionosphere models. Figure taken from *Fox* [2007].

ing the VTS3 model, the ONMS densities were normalized by a factor of 1.63, which was indicated by a comparison of the ONMS densities to those measured by the Entry Probes and the BNMS.

[3] The VTS3 model uses a spherical harmonic expansion up to order 5 with first-order variations in solar zenith angle, while latitude and local time terms introduce a small second-order asymmetric variation. The models are based on a mean F10.7 index of 200 for the first two diurnal cycles. The densities in the terminator regions were difficult to incorporate into the model because of the steep gradients in density and the low order of the polynomials used. Also, the VTS3 model is most accurate for low latitudes, and fairly high solar activity [*Hedin et al.*, 1983].

[4] The ONMS data without the normalizing factor of 1.63 were placed in the Planetary Data System (PDS) and into the PV Unified Abstract Data System (UADS). The UADS consisted of three databases, one of which was the Low Frequency Data, the purpose of which was to facilitate comparison of different in situ measurements at 12 s intervals. Goddard Space Flight Center generated a version of this database for the first 1000 orbits for use by the ONMS, the Orbiter Electron Temperature Probe (OETP) [e.g., *Brace et al.*, 1980, and references therein], and the Orbiter Ion Mass Spectrometer (OIMS) [e.g., *Taylor et al.*, 1980].

[5] The mass densities measured by the PV Orbiter Atmospheric Drag (OAD) experiment, and reported by, for example, *Keating et al.* [1980], were also larger than the ONMS data by about 60%. For the Venus International Reference Atmosphere (VIRA), *Keating et al.* [1985] suggested that the ONMS density data for CO_2 should be multiplied by a factor 1.83, and that of O should be multiplied by a factor of 1.58 in order for the ONMS data to be consistent with the OAD mass density data. For the 150 to 250 km region, however, the VIRA suite of models comprised only one model for 10:00 and 14:00 local times on the dayside, one model for the terminators, and one model for the nightside at 02:00 and 22:00 hours. For the altitude range of 100 to 150 km, only one dayside and one nightside model were given. Thus a comparison between the VTS3 and VIRA models in the near-terminator region is not possible.

[6] The PV Orbiter Radio Occultation (ORO) experiment provided electron density profiles throughout the 14 years of the mission, which encompassed the whole range of solar zenith angle and solar activity (see the reviews by, for example, *Kliore and Mullen* [1989], *Kliore* [1992], and *Fox and Kliore* [1997]). Although the early ORO electron density profiles used in this study were measured at high latitudes, the in situ data were measured in the near equatorial region.

[7] *Fox* [2007] has recently modeled the Venus ionosphere in the near terminator region for solar zenith angles from 60 to 85° in 5° increments and from 86 to 90° in 1° increments, using the VTS3 model in the dusk sector for an average $F_{10.7}$ of 200. The altitudes of the model peaks as a function of SZA in the near terminator region are reproduced in Figure 1. The major ion at the (upper) F_1 peak in the electron density profiles is produced by photoionization and, to a somewhat lesser extent, by photoelectron impact ionization of CO_2, to produce CO_2^+, which is then transformed to O_2^+ by reaction with O. There is also some contribution from production of O^+, both from direct ionization of O and from dissociative ionization of CO_2, which, in the photochemical equilibrium region, is transformed also to O_2^+ by reaction with CO_2. O_2^+ is destroyed mostly by dissociative recombination,

$$O_2^+ + e \rightarrow O + O, \tag{1}$$

although at very low altitudes O_2^+ may also react with NO and N to produce NO^+. Details of the models are given by *Fox* [2007].

[8] *Fox* [2007] found that, in fairly good agreement with PV ORO data and other models, the relative magnitudes of the total ion density peaks were approximately Chapman-like, but the altitudes of the model peaks remained near 140–141 km from 60 to 80° SZA. For solar zenith angles from 85 to 90°, the model peak rose abruptly from 144 to 149 km. Thus the altitude of the peak, z_m, was predicted to rise with increasing SZA (χ), but not quite as rapidly as *Chapman* [1931a] theory would suggest:

$$z_m = z_0 + H \ln \sec(\chi). \tag{2}$$

In this equation z_0 is the altitude of the subsolar ($\chi = 0°$) peak electron density, and H is the neutral scale height near the peak, which is in the range ~5–10 km in the 140 to 160 km region of our models. In the near terminator region, this equation breaks down because the secant of the SZA becomes infinite at 90°. Either a Chapman function [e.g., *Chapman*, 1931b] must be substituted for the secant, or, for more accuracy, the densities along the line of sight to the sun for a given altitude and SZA can be integrated numerically, as described, for example, by *Rees* [1989]. The ratio of this integrated density to the value of the

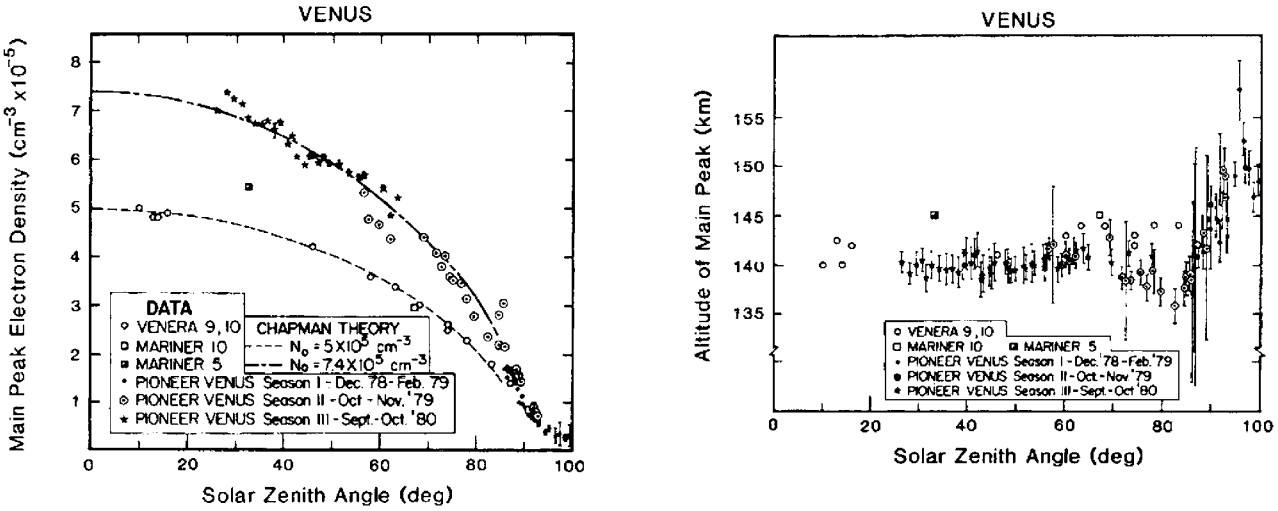

Figure 2. Peak electron densities and altitudes for the F_1 peaks as a function of solar zenith angle from the PV ORO and other radio occultation data. (left) Peak densities as a function of SZA. The curves through the data are the best fits to Chapman equations for low and high solar activities. (right) Peak altitudes as a function of SZA for radio occultation data. Figure taken from *Cravens et al.* [1981].

integrated overhead (column) densities forms an "effective secant." The "effective secant", which is altitude dependent, begins to diverge from the actual secant on Venus near 80° SZA, and the deviation becomes larger for larger solar zenith angles. For example, in the model of *Fox* [2007], at 90° solar zenith angle, the value of the number densities integrated along the line of sight to the sun above an altitude of 140 km is 3.9×10^{17} cm^{-2}, compared to an integrated overhead density of 1.0×10^{16} cm^{-2}. Thus the ratio and "effective secant" is 39 for our 90° SZA model at 140 km.

[9] *Cravens et al.* [1981] investigated the electron density profiles measured by the PV ORO from 1978 December to 1980 October, and plotted the altitudes and magnitudes of the peaks as a function of solar zenith angle for these data as well as those of Mariner 5 [e.g., *Kliore et al.*, 1967; *Mariner Stanford Group*, 1967], Mariner 10 [e.g., *Howard et al.*, 1974; *Fjeldbo et al.*, 1975], and Venera 9 and 10 [e.g., *Ivanov-Kholodny et al.*, 1979]. Except for the profiles from Veneras 9 and 10, all these data were obtained during moderately high to very high solar activity. Plots of the magnitudes and altitudes of the peaks as a function of solar zenith angle from *Cravens et al.* [1981] are reproduced here as Figure 2. Although the measured magnitudes of the peaks behave in a nearly Chapman-like manner, the altitude of the peak can be seen to be approximately constant at 140 km for solar zenith angles ranging from ~25 to 70°. *Cravens et al.* [1981] explained the nearly constant altitude of the peak over such a large solar zenith angle range as owing to the "collapse" of the thermosphere as it merges into the nightside cryosphere, where the temperature and densities are very low. The model calculations of *Fox* [2007] shown in Figure 1 predicted that the altitude of the peak was approximately constant for the 60° to 80° SZA models, as would be expected. A decrease in the altitude of the peak to about 135 km, however, appears in the PV radio occultation data for solar zenith angles from 70 to 85°, which the models of *Fox* [2007] do not reproduce. (It is worth noting that the low solar activity Venera data do not, however, exhibit this decrease.) *Fox* [2007] tentatively attributed this discrepancy to known inadequacies of the VTS3 model. *Hedin et al.* [1983] state specifically that rapid terminator changes in the densities cannot be faithfully represented in the VTS3 model. The simplest explanation therefore was that the actual neutral densities in the 75–85° SZA range were smaller than those computed with the VTS3 model. *Fox* [2007] showed that, if the densities taken from the VTS3 model for an 85° SZA were decreased by a uniform factor of 2, the peak appeared lower by ~4 km.

[10] Other possible factors are that the values of the electron temperatures, T_e, and its gradients are smaller than those we have assumed in our models. We do not discuss this possibility here; the changes would have to be large, and our model values of T_e reproduce fairly well the empirical models of *Theis et al.* [1980, 1984]. Increases in solar activity will also tend to lower the altitude of the electron density peak, if the background neutral atmosphere is assumed to be the same. This effect results from the change in shape of the ionizing EUV and soft X-ray regions of the solar spectra, which are characterized by larger enhancements in the shorter wavelength region from low to high solar activity. The absorption cross sections at shorter wavelengths are generally smaller than those at longer wavelengths, which results in deeper penetration of the ionizing solar fluxes. We do not, however, expect this to be a major factor here since all the PV ORO data presented by *Cravens et al.* [1981] were at fairly high solar activity.

[11] A sharp increase in the F_1 peak altitude is seen in the PV ORO data in Figure 2 for solar zenith angles greater than 85°; for solar zenith angles of 90–96°, the peak altitude appears in the range of ~147 to 157 km, with error bars of 1–2 km [*Cravens et al.*, 1981]. In the 90° SZA model of *Fox* [2007], the electron density peak is near 149 km. Although this altitude is slightly higher than the data show, it is in acceptable agreement. We investigate here

Table 1. Characteristics of the PV Orbits

Orbit Number	Date[a]	Local Time, hours	SZA,[b] degrees	$F_{10.7}$[c]
		Dawn Orbits		
133	79106	6.3	85.5	169.6
134	79107	6.4	84.0	173.0
135	79108	6.5	82.3	170.0
137	79110	6.7	79.4	175.8
138	79111	6.8	77.9	170.9
139	79112	6.9	76.4	168.1
140	79113	7.0	74.8	170.7
141	79114	7.1	73.3	168.0
361	79335	6.7	79.6	189.8
363	79337	6.9	76.6	184.2
		Dusk Orbits		
234	79207	17.0	76.6	153.4
235	79208	17.1	78.2	152.8
236	79209	17.3	79.8	144.2
237	79210	17.4	81.3	149.3
238	79211	17.5	82.9	150.0
239	79212	17.6	84.5	155.6
457	80066	16.9	74.8	172.9
459	80068	17.1	78.0	172.7
460	80069	17.2	79.6	171.8
461	80070	17.4	81.1	169.4
462	80071	17.5	82.7	166.3
463	80072	17.6	84.3	164.9

[a]The date is expressed in the form YYDDD, where YY is the last two digits of the year and DDD is the ordinal day of the year. For example, 79106 is day 106 of year 1979.
[b]Solar zenith angle.
[c]Corrected for the orbital position of Venus with respect to that of the Earth.

the source of the apparently sudden decrease in the altitudes of the main peak between 75 and 85° SZA at high solar activity.

2. Comparison With the VTS3 Models

[12] First, we have investigated whether the ONMS measured densities of O and CO_2 were smaller than those of the VTS3 model in this SZA range, which would explain the lower altitudes of the measured F_1 electron density peaks as compared to the model peaks shown in Figure 1. We have selected PV orbits for which the O and CO_2 density profiles were measured by the ONMS and reported in UADS data base, and which were characterized by solar zenith angles from 75 to 85°. We have compared them to the densities derived from the VTS3 model for the same conditions. We have identified 10 orbits (133–135, 137–141, 361, and 363) in the dawn sector, and 12 orbits (234–239, 457, and 459–463), in the dusk sector which met these criteria. The characteristics of each of the 22 orbits are shown in Table 1. There were also several orbits, such as 8–14, 136, 362, and 458, for which the solar zenith angles were in the appropriate range, but for which the O and/or CO_2 density profiles were not available in the UADS database.

[13] In Figures 3 to 6 we present the O and CO_2 density profiles from the ONMS data for the selected orbits, along with those of the VTS3 model for the same hour angle, solar zenith angle, and $F_{10.7}$. The values of $F_{10.7}$ were adjusted for the orbital position of Venus with respect to that of the Earth. We plot the O and CO_2 density profiles, suitably normalized by the factor 1.63, for both the inbound and outbound legs of the orbits. The outbound legs were more vertical than the inbound legs and are therefore less subject to effects due to spherical asymmetry. The results are plotted from 140 to 200 km. These individual parts of Figures 3–6 are labeled by the PV orbit number and the solar zenith angle at periapsis. The densities from the VTS3 model are represented by the solid curves, those from the inbound legs of the orbits by the dotted curves, and those outbound legs by the dashed curves.

[14] In Figures 3 and 4 we show the density profiles for six and four orbits, respectively, in the dawn sector. The grouping of the orbits into two figures is for display purposes, and has no other significance. These figures show that the CO_2 densities measured by the ONMS on the outbound segments of the orbits are generally larger than those generated by the VTS3 models by a factor of ~2. By contrast, except for orbit 361, there is significant agreement between the O density profiles from the outbound parts of the orbits and those of the VTS3 models, which are only slightly larger at high altitudes, and slightly smaller at lower

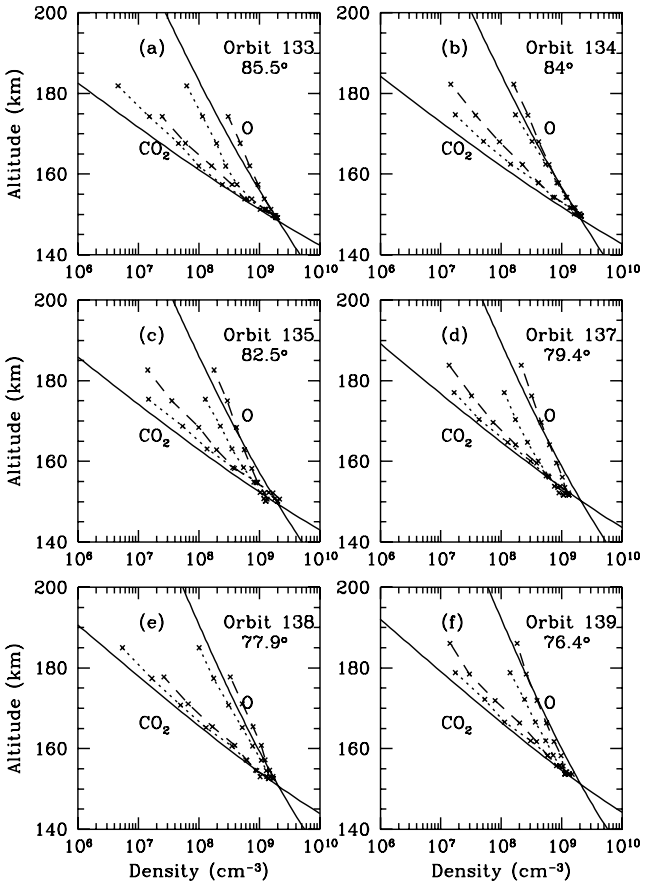

Figure 3. Number densities of O and CO_2 as a function of altitude for PV dawn Orbits 133 to 135 and 137 to 139. The densities computed with the VTS3 model are shown as solid curves. The densities measured by the ONMS, which are taken from the UADS database and normalized by the factor 1.63 [e.g., *Hedin et al.*, 1983], for the inbound and outbound legs of the orbits are shown as dotted and dashed curves, respectively. Each part of the figure is labeled with the orbit number and the solar zenith angle at periapsis.

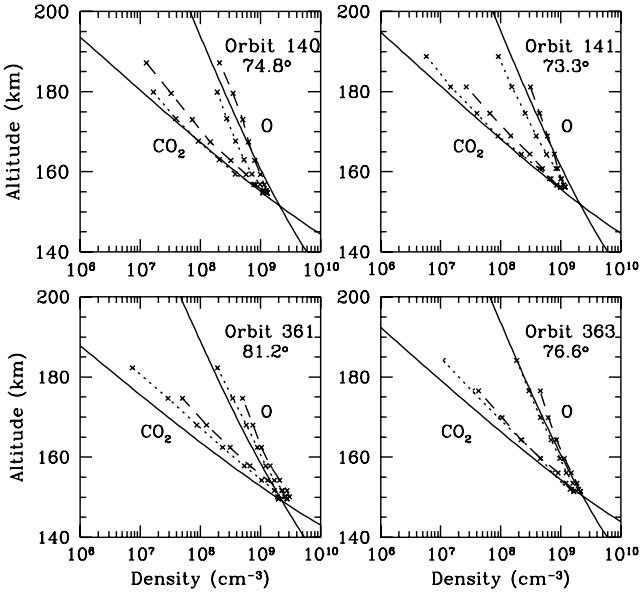

Figure 4. Same as Figure 3, but for dawn orbits 140, 141, 361, and 363.

altitudes. The O densities from the inbound portions of the orbits are slightly smaller than those of the VTS3 model.

[15] In Figures 5 and 6, we show the results for twelve orbits in the dusk sector. These figures generally show that, with the exception of Orbit 234, and to a lesser extent orbit 459, both the O and CO_2 densities computed using the VTS3 model are significantly smaller than those of the normalized ONMS densities.

[16] We have interpolated the normalized ONMS O and CO_2 densities from the outbound parts of the orbits to 165 km, and compared them to the VTS3 model number densities at 165 km in Table 2. The measured and model O densities are generally in agreement to within a factor of 2 or less. The disagreement between the CO_2 measured and model densities is somewhat greater, with noticeably larger measured densities than those generated by the VTS3 models.

3. Dawn/Dusk Asymmetries

[17] It is apparent that the discrepancy between the altitudes of the measured peaks in the electron density profiles and the modeled values in the 75 to 85° SZA range cannot be explained as arising from known inadequacies of the VTS3 model in the near terminator region. In fact, we found that most of the ONMS measured densities were larger, rather than smaller, than those of the VTS3 model. Smaller densities would be required for the peak electron density to appear below 140 km in the 75–85° SZA region.

[18] It is noteworthy, however, that most of the VTS3 models for the dawn thermospheres are similar to each other, those of the dusk thermospheres are similar to each other, and there is a clear dawn/dusk asymmetry between the model neutral density profiles at altitudes above 170 km. This is evident when the dawn neutral density profiles, which are shown in Figures 3 and 4 are compared to those of the dusk profiles, which are shown in Figure 5 and 6. A careful examination of Figure 2 from *Cravens et al.* [1981] shows that the low-altitude peaks from ~70 to ~85° SZA are all from PV ORO season II, which corresponded to dates between 1979 October and November, and to high to very high solar activity. The orbits with peak altitudes below 140 km were all at high latitudes, and periapses of these orbits are all in the pre-dawn and dawn sector. Although no information is available about the local time of PVO ORO profiles, it is likely that if periapsis of an orbit is in the dawn sector, the ORO profiles were in the same sector (A. Kliore, personal communication, 2007). We have therefore examined the possibility that the decrease in altitude of the ionospheric peak in the 75 to 85° SZA range is actually due to a dawn/dusk asymmetry between the neutral density profiles.

[19] *Niemann et al.* [1980] and *Hedin et al.* [1983] presented diurnal variations of the He, N, O, N_2, CO, and CO_2 densities as a function of local time at altitudes of 157 and 167 km. These plots show that the greatest asymmetry between the densities was in the pre-dawn and post-dusk regions, and was greater for the lighter species than the heavier species. *Niemann et al.* [1980] concluded that, in the altitude and latitude range that they investigated, the dayside densities of species other than helium behave quite regularly, showing approximate symmetry about local noon. For the Venus International Reference Atmosphere, *Keating et al.* [1985] suggested that, in the 150–250 km range, there were

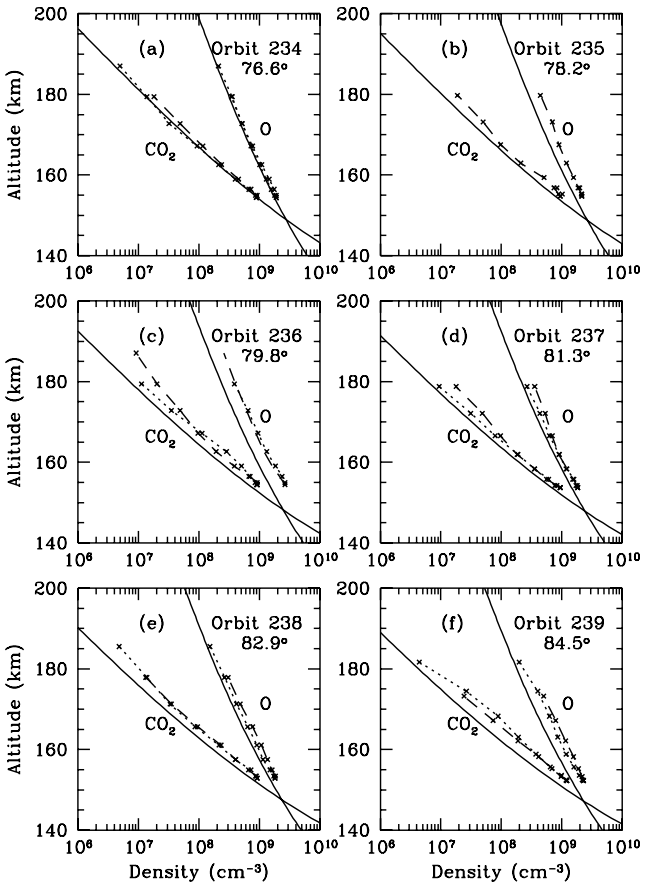

Figure 5. Same as Figure 3, but for dusk orbits 234–239. Notice that for Orbit 235, the densities from the inbound portion of the orbit are available only at 2 points near periapsis.

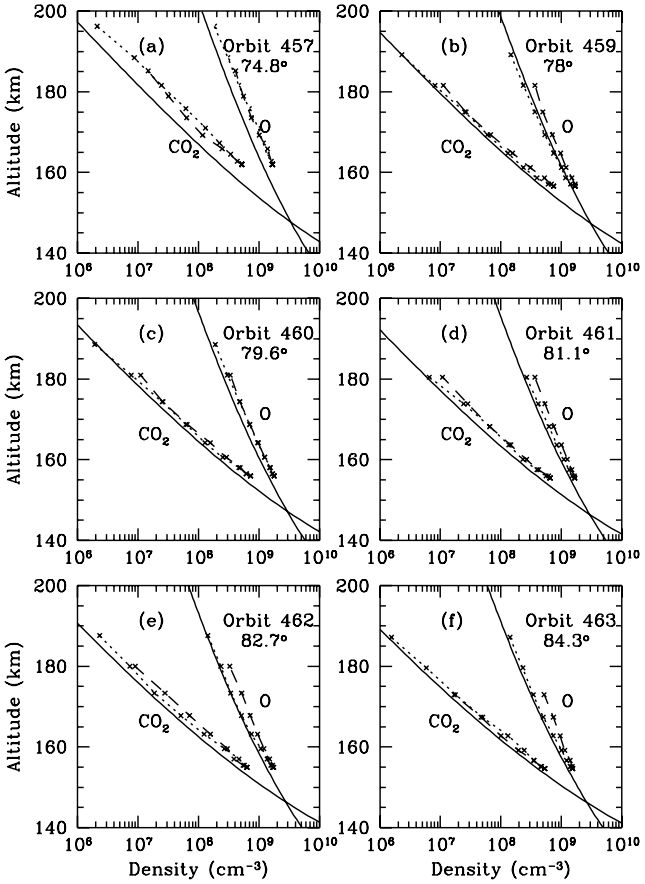

Figure 6. Same as Figure 3, but for dusk orbits 457 and 459–463.

small local time asymmetries in the thermospheric densities but the strongest asymmetries were in the densities of the light species H and He, which we do not expect to affect the altitude or magnitude of the peak electron density. The exospheric temperatures, however, derived from the scale heights of the neutral density profiles were significantly larger in the evening than in the morning, and minimized in the pre-dawn region.

[20] In Figure 7 we present the VTS3 model altitude density profiles of CO_2 and O for high solar activity ($F_{10.7}$ = 175) and solar zenith angles of 75, 80 and 85° in the equatorial dawn and dusk sectors. The density profiles are roughly equal for the six models for both O and CO_2 up to ~165 km. The densities of O exceed those of CO_2 at altitudes that range from 146 to 151 km for all the models. Above about 165 km, the densities are larger in the dusk sector than the dawn sector, and the densities decrease as the solar zenith angle increases from 75 to 80 to 85°, as one might expect. Thus, at altitudes above ~170 km, there is a clear dawn/dusk asymmetry. The exospheric temperatures for the VTS3 75, 80° and 85° SZA dawn models are 263, 244 K and 228 K, respectively, and those for the dusk models are 313, 311 and 304 K, respectively. Since there is no dawn/dusk asymmetry at altitudes within ~20 km (about 3 scale heights) above the expected altitude of the peaks at ~135–140 km, however, we do not expect that the high-altitude dawn/dusk asymmetry will produce significantly different model ion or electron density profiles.

[21] In Figure 8 we show the major neutral density profiles for model thermospheres based on the 80° dawn and dusk equatorial VTS3 models. Although the O densities are clearly smaller for the dawn model near 200 km, there is little difference in the densities below ~165 km. Just as we showed in Figure 7, the thermospheric densities are invariant up to quite high altitudes. The most apparent differences in composition between the dawn and dusk 80° SZA model thermospheres are that the dusk H densities at 175 km (~1×10^5 cm^{-3}) are smaller than those at dawn (~4×10^5 cm^{-3}) [cf. *Grebowsky et al.*, 1995], and that near 200 km the density of He in the dawn model, 3.2×10^6 cm^{-3}, is more than twice that in the dusk model, 1.48×10^6 cm^{-3}. Above 400 km in the VTS3 model, however, the dawn/dusk asymmetry in the He densities is reduced to less than ~16%.

[22] In Figure 9, we present model ionospheres for the 80° SZA dawn and dusk regions. The He^+ and H^+ densities are clearly larger at high altitudes in the dawn than in the dusk ionospheres. The electron density peak in the dawn ionosphere is 2.8×10^5 cm^{-3} at 142 km. For the dusk ionosphere, the electron density peak is 2.7×10^5 cm^{-3} at 141 km. Thus we find that the large dawn/dusk asymmetry in the temperatures and densities at high altitudes does not significantly affect the altitude or magnitude of the electron density peak.

[23] Since periapsis of the PV orbiter was rarely below 150 km, it is possible that there is a dawn/dusk asymmetry in the lower thermospheric densities that is not reflected in the VTS3 models. As we showed in Figure 7, the VTS3 model predicts that the density profiles for dawn and dusk at

Table 2. Measured and Model Number Densities for O and CO_2 at 165 km, cm^{-3}

PV Orbit Number	O Density Measured[a]	O Density VTS3[b]	CO_2 Density Measured[a]	CO_2 Density VTS3[b]
		Dawn Orbits		
133	5.72(8)[c]	4.44(8)	9.65(7)	4.16(7)
134	5.14(8)	4.81(8)	1.49(8)	5.22(7)
135	5.00(8)	5.16(8)	1.52(8)	6.43(7)
137	5.97(8)	6.01(8)	1.51(8)	9.53(7)
138	8.08(8)	6.38(8)	1.80(8)	1.13(8)
139	6.07(8)	6.77(8)	2.43(8)	1.32(8)
140	7.23(8)	7.25(8)	2.23(8)	1.54(8)
141	7.49(8)	7.63(8)	2.76(8)	1.78(8)
361	8.96(8)	5.89(8)	2.07(8)	7.73(7)
363	8.11(8)	7.16(8)	1.99(8)	1.29(8)
		Dusk Orbits		
234	8.47(8)	8.12(8)	1.63(8)	1.38(8)
235	1.06(9)	7.55(8)	1.50(8)	1.21(8)
236	1.01(9)	6.39(8)	1.35(8)	8.98(7)
237	7.55(8)	5.97(8)	1.20(8)	7.80(7)
238	8.01(8)	5.53(8)	1.08(8)	6.69(7)
239	9.38(8)	5.15(8)	1.11(8)	5.77(7)
457	1.44(9)	9.22(8)	2.92(8)	1.35(8)
459	9.38(8)	7.84(8)	1.51(8)	1.06(8)
460	9.19(8)	7.18(8)	1.34(8)	9.17(7)
461	9.21(9)	6.57(8)	1.15(8)	7.51(7)
462	8.65(8)	6.06(8)	1.17(8)	6.41(7)
463	8.42(8)	5.53(8)	6.95(8)	5.47(7)

[a]From the PV ONMS UADS data for the outbound legs of the orbits multiplied by the normalization factor of 1.63, and interpolated to 165 km.
[b]As calculated using the VTS3 model of *Hedin et al.* [1983].
[c]Read as 5.72×10^8.

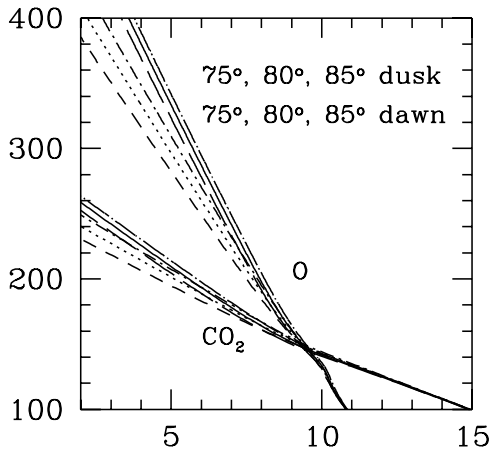

Figure 7. O and CO_2 density profiles from the VTS3 model for near equatorial 75, 80, and 85° dawn and dusk conditions. The dot-long-dashed, solid, and long-dashed curves represent the 75, 80, and 85° dusk profiles, respectively. The dot-short-dashed, dotted, and short-dashed curves represent the 75, 80, and 85° dawn profiles, respectively.

75, 80 and 85° SZA merge below about 165 km for both O and CO_2. If there were a significant dawn/dusk asymmetry in the O and CO_2 density profiles between 135 km and 155–165 km, however, a noticeable difference between the model electron density peak altitudes would result.

[24] *Alexander et al.* [1993] examined images from the PV Orbiter Ultraviolet Spectrometer (OUVS) at 130 nm to study the structure and dynamics of the Venus thermosphere over the period 1980–1990. The OI triplet emission features at 130.2, 130.4, and 130.6 nm arise from the $O(^3S^o \rightarrow {}^3P_{2,1,0})$ transition; they are produced by electron impact excitation of O and by resonance scattering of sunlight. *Alexander et al.* [1993] modeled the data, including radiative transfer. They assumed that the CO_2 profiles were constant and varied the O mixing ratio to fit the observed emissions. They found a local time asymmetry in the O emissions at latitudes above 30°, which they interpreted as resulting from a reduction by a factor of 2 in the O mixing ratios in the dawn sector. They explained this as arising from a difference in the supply of gravity waves from the middle atmosphere, which provides an asymmetry in the turbulent mixing. This mixing would tend to transport O (and presumably other minor species) downward more efficiently and reduce the O mixing ratios. The local time asymmetry disappears at equatorial latitudes, where the VTS3 model is most accurate. The list of ORO orbits given by *Cravens et al.* [1981] from 1979 October to November shows that the peaks that fall below 140 km in the 70 to 85° range were indeed all at high northern latitudes.

[25] Gravity waves propagating vertically between 100 and 150 km deposit energy that is asymmetric in local time and act to couple the lower and upper thermosphere. Evidence for such waves has been presented by, for example, *Kasprzak et al.* [1993], who observed wave-like perturbations in the ONMS density profiles during the entry phase of the PV Orbiter in late 1992. These waves are consistent with gravity waves propagating upward from the lower thermosphere. The wave amplitudes have a breaking level in the 140 to 150 km region [*Bougher et al.*, 1988; *Kasprzak et al.*, 1993].

[26] Using the Venus Thermospheric General Circulation Model (VTGCM) that includes superrotating winds, *Bougher and Borucki* [1994] and *Zhang et al.* [1996] showed that the winds are stronger across the evening terminator than across the morning terminator. The superrotation of the thermosphere, a mechanism for which was put forward by *Alexander* [1992], explains the observed offset toward the morning terminators of the O_2 and NO nightglow emissions, which are produced by the recombination of O and N transported from the dayside to the nightside. In addition, these winds smooth out the densities of species such as O and N over the evening terminator. Thus the VTGCM predicts that the densities of minor neutral densities do not change as rapidly across the evening terminator as they do across the morning terminator.

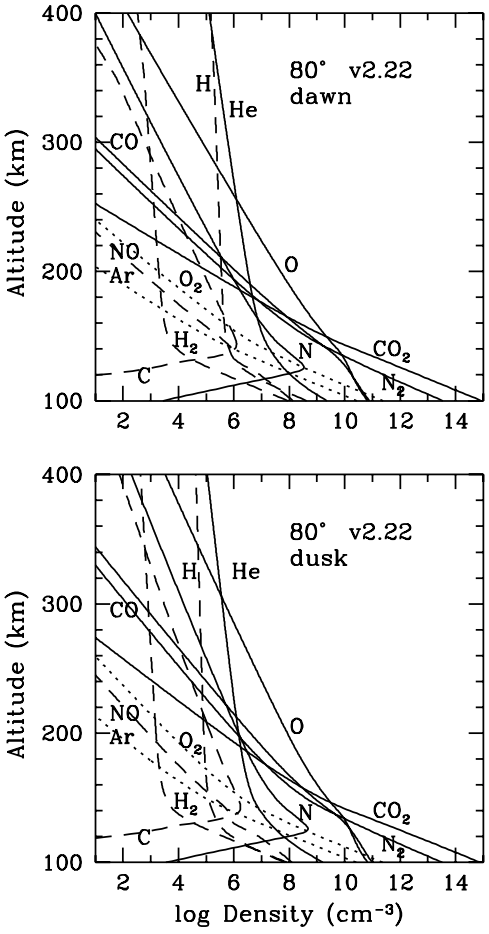

Figure 8. Altitude profiles for 12 neutral species for the 80° thermospheric models: (top) the dawn model and (bottom) the dusk model. The solid curves are density profiles taken from the VTS3 model. The dashed curves are for H and H_2 density profiles; the dotted curves are for NO, C, Ar, and O_2, which were computed self-consistently in the models. "v2.22" refers to the Solar 2000 v2.22 solar flux model of *Tobiska* [2004], which was used in constructing the thermosphere/ionosphere models. Details of the neutral models are given by *Fox* [2007].

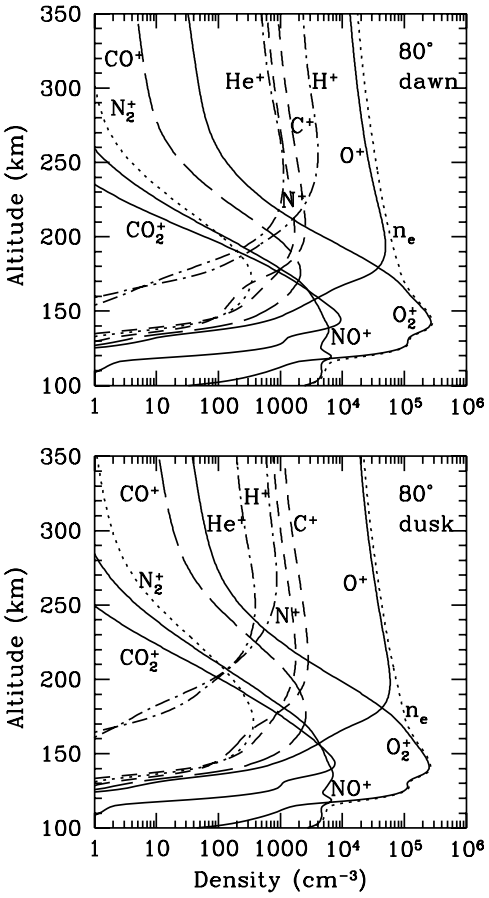

Figure 9. Altitude density profiles for 10 ions for the 80° ionospheric models: (top) the dawn model and (bottom) the dusk model. The O_2^+, CO_2^+, and NO^+ profiles are shown as solid curves, the CO^+ profiles are shown as a long-dashed curve, the C^+ and N^+ profiles are shown as short-dashed curves, and the H^+ and He^+ profiles are shown as dot-dashed curves. The total electron density profile is shown as a dotted curve.

[27] We find, however, that decreasing only the O densities (or mixing ratios) cannot explain the lower peaks in the ionospheres. We have done a test calculation in which we reduce the O and CO densities by a factor of 2 in the 80° SZA model. The results of this model suggest that the altitude of the peak is reduced by only 2 km, from 141 km to 139 km. While this reduction is significant, the altitude of the peak could be further reduced only if the densities of the major species CO_2 are also smaller within about 20 km above the peak altitude. Such a variation in the densities could be produced by an asymmetry in the neutral temperatures above the electron density peak altitude. Smaller neutral temperatures lead to smaller neutral scale heights. The altitude of the peak is near optical depth unity, i.e., where $\tau \approx \sigma nH = 1$. In this equation, σ is the absorption cross section, and n is the neutral density. If H decreases, the photon energy will be deposited at larger neutral densities, and thus at lower altitudes. We suggest therefore that the most likely explanation for the lower electron density peak altitudes is that the scale heights associated with the neutral density profiles are smaller due to dawn/dusk variations in the temperatures at high latitudes. Slightly lower temperatures (by 1 to 9 K) in the 130 to 160 km region have been predicted by the VTGCM [e.g., *Bougher et al.*, 1994; *Zhang et al.*, 1996]. Details of the lower-temperature profiles required by the models to fit the altitudes of the ionospheric peaks depend on assumptions about boundary conditions, eddy diffusion coefficients and the other density profiles, and further refinements in the conclusions are beyond the scope of this work.

4. Conclusions

[28] We have investigated the difference between the measured and model neutral density profiles in the Venus thermosphere, with a view toward explaining the ~4–5 km dip below 140 km in the altitude of the electron density peaks as measured by the PV ORO between 75° and 85° SZA, which is illustrated here in Figure 2 from *Cravens et al.* [1981]. Of the first 600 orbits, we have identified 10 and 12 orbits in the UADS data base in the dawn and dusk sectors, respectively, for which the SZA ranged from 75 to 85°. We find that the normalized ONMS densities are roughly equal to or larger than those of the VTS3 model. In the dawn sector, the CO_2 densities are larger than those derived from the VTS3 model, but there is fairly good agreement between the measured O densities and those of the normalized ONMS data. The normalized ONMS densities in the very near terminator region exhibit similar or larger, rather than smaller densities, by factors of up to ~2, and therefore the difference between the densities measured by the ONMS and the VTS3 model densities cannot explain the lower altitude of the electron density peaks in this SZA range. Model studies by *Fox* [2007] showed that a 4–5 km dip in the electron density peak requires a factor of 2 reduction in all the neutral densities in the model.

[29] Because the VTS3 model employed only a small number of spherical harmonics, it was not expected to reproduce accurately the neutral densities across the terminators, where they are expected to change rapidly as the thermosphere merges into the nightside cryosphere [*Hedin et al.*, 1983]. In addition, the VTS3 model is expected to be most accurate at high solar activity and in the low-latitude region where the bulk of the in situ measurements were made.

[30] The radio occultation electron density peaks in the 70–85° SZA range, as reported by *Cravens et al.* [1981], are all in the dawn sector and at high latitudes. Thus it is possible that there is a dawn/dusk asymmetry that is not reflected in the VTS3 model near and above the ion peak. We did find a dawn/dusk asymmetry in the exospheric temperatures and densities above 165 km, with considerably smaller values in the dawn sector. In the VTS3 models, the temperature and density differences do not, however, extend to below about 165 km, which is the most important region in determining the altitude of a peak in the 135–140 km region. The high-altitude asymmetry, as expressed by the VTS3 models, cannot explain the lower peak altitudes in the 75 to 85° SZA range. The near equality of the VTS3 densities below an altitude of 165 km, however, may be an artifact of the assumptions embedded in the model.

[31] *Alexander et al.* [1993] found a local time asymmetry, which was confined to latitudes above 30°, in the atomic

oxygen 130 nm intensities, as measured by the PV OUVS. They suggested that this asymmetry could result from a high-latitude dawn/dusk asymmetry in the O densities, with values at the dawn terminator that were a factor of 2 smaller than those at the evening terminator. They interpreted this as due to the upward propagation of gravity waves, which produces a pattern of turbulence that is asymmetrical in local time. Evidence for such gravity waves in the ONMS data has been presented by, for example, *Kasprzak et al.* [1993]. Although they were not able to reproduce the findings of *Alexander et al.* [1993], *Bougher and Borucki* [1994], and *Zhang et al.* [1996] found morning/evening asymmetries in the temperatures and densities due to the superrotation of the thermosphere.

[32] We therefore suggest that the low-altitude ion peaks between ~70 and ~85° shown in the investigation of *Cravens et al.* [1981], are produced by a dawn/dusk asymmetry that may be confined to high latitudes, in the neutral temperatures and the major neutral densities (CO_2, O, CO, and N_2) within about 2–3 scale heights above the expected peak height, near 135 km. A reduction by a factor of 2 of the mixing ratio of O (which was suggested by *Alexander et al.* [1993]) and CO in the models, was found to reduce the altitude of the ion peak by only about 2 km. A further lowering of the altitude of the peak electron density profiles could only be accomplished by a reduction in the CO_2 density profile at high latitudes in the dawn sector. This reduction could arise from smaller neutral temperatures immediately above the electron density peak in the high-latitude dawn sector than those predicted by the VTS3 model. Such an asymmetry has implications for the dynamics of the thermosphere, including superrotation, for the global distribution of airglow emissions and, from an engineering perspective, for aerobraking of spacecraft in the Venus thermosphere.

[33] **Acknowledgments.** We thank T. E. Cravens for suggesting this study. This work has been supported by grants NAG5-12755 and MAG5-13313 from the National Aeronautics and Space Administration.

References

Alexander, M. J. (1992), A mechanism for the Venus thermospheric superrotation, *Geophys. Res. Lett.*, *19*, 2207–2210.

Alexander, M. J., A. I. F. Stewart, S. C. Solomon, and S. W. Bougher (1993), Local time asymmetries in the Venus thermosphere, *J. Geophys. Res.*, *98*, 10,849–10,871.

Bougher, S. W., and W. J. Borucki (1994), Venus O_2 visible and IR nightglow: Implications for lower thermosphere dynamics and chemistry, *J. Geophys. Res.*, *99*, 3759–3776.

Bougher, S. W., R. E. Dickinson, E. C. Ridley, and R. G. Roble (1988), Venus mesosphere and thermosphere, III Three-dimensional general circulation with coupled dynamics and composition, *Icarus*, *73*, 545–573.

Bougher, S. W., D. M. Hunten, and R. G. Roble (1994), CO_2 cooling in terrestrial planet thermospheres, *J. Geophys. Res.*, *99*, 14,609–14,622.

Brace, L. H., R. F. Theis, W. R. Hoegy, J. H. Wolfe, J. D. Mihalov, C. T. Russell, R. C. Elphic, and A. F. Nagy (1980), The dynamic behavior of the Venus ionosphere in response to solar wind interactions, *J. Geophys. Res.*, *85*, 7663–7678.

Chapman, S. (1931a), The absorption and dissociative or ionizing effects of monochromatic radiation in an atmosphere of a rotating earth, *Proc. Phys. Soc. London*, *43*, 26–45.

Chapman, S. (1931b), The absorption and dissociative or ionizing effects of monochromatic radiation in an atmosphere of a rotating earth. Part II. Grazing incidence, *Proc. Phys. Soc. London*, *43*, 483–501.

Cravens, T. E., A. J. Kliore, J. U. Kozyra, and A. F. Nagy (1981), The ionospheric peak on the Venus dayside, *J. Geophys. Res.*, *86*, 11,323–11,329.

Fjeldbo, G., B. Seidel, D. Sweetnam, and H. T. Howard (1975), The Mariner 10 radio occultation measurements of the ionosphere of Venus, *J. Atmos. Sci.*, *32*, 1232–1236.

Fox, J. L. (2007), Near-terminator Venus ionosphere: How Chapman-esque?, *J. Geophys. Res.*, *112*, E04S02, doi:10.1029/2006JE002736.

Fox, J. L., and A. J. Kliore (1997), Ionosphere: Solar activity variations, in *Venus II*, edited by S. Bougher, D. Hunten, and R. Phillips, pp. 161–188, Univ. of Ariz. Press, Tucson.

Grebowsky, J. M., W. T. Kasprzak, R. E. Hartle, and T. M. Donahue (1995), A new look at Venus thermosphere H distribution, *Adv. Space Res.*, *17*(11), 191–195.

Hedin, A. E., H. B. Niemann, W. T. Kasprzak, and A. Seiff (1983), Global empirical model of the Venus thermosphere, *J. Geophys. Res.*, *88*, 73–83.

Howard, H. T., et al. (1974), Venus: Mass, gravity field, atmosphere, and ionosphere of Venus as measured by the Mariner 10 dual-frequency radio system, *Science*, *183*, 1297–1301.

Ivanov-Kholodny, G. S., et al. (1979), Daytime ionosphere of Venus as studied with Veneras 9 and 10 dual-frequency radio occultation measurements, *Icarus*, *39*, 209–213.

Kasprzak, W. T., H. B. Niemann, and A. E. Hedin (1993), Wave like perturbations observed at low latitudes by the Pioneer Venus orbiter neutral mass spectrometer during orbiter entry, *Geophys. Res. Lett.*, *23*, 2755–2758.

Keating, G. M., J. Y. Nicholson, and L. R. Lake (1980), Venus upper atmosphere structure, *J. Geophys. Res.*, *85*, 7941–7956.

Keating, G. M., et al. (1985), Models of the Venus neutral upper atmosphere: Structure and composition, *Adv. Space Res.*, *5*(11), 117–171.

Kliore, A. J. (1992), Radio occultation observations of the ionospheres of Mars and Venus, in *Venus and Mars: Atmospheres, Ionospheres, and Solar Wind Interaction*, *Geophys. Monogr. Ser.*, vol. *66*, pp. 265–276, edited by J. G. Luhmann, M. Tatrallyay, and R. Pepin, AGU, Washington, D. C.

Kliore, A. J., and L. F. Mullen (1989), Long term behavior of the main peak of the dayside ionosphere of Venus during solar cycle 21 and its implications on the effect of the solar cycle upon the electron temperature in the main peak region, *J. Geophys. Res.*, *94*, 13,339–13,351.

Kliore, A. J., G. S. Levy, D. L. Cain, G. Fjeldbo, and S. I. Rasool (1967), Atmosphere and ionosphere of Venus from the Mariner 5 S-band radio occultation measurements, *Science*, *205*, 99–102.

Mariner Stanford Group (1967), Ionosphere and atmosphere as measured by dual-frequency radio occultation of Mariner V, *Science*, *158*, 1678–1683.

Niemann, H. B., W. T. Kasprzak, A. E. Hedin, D. M. Hunten, and N. W. Spencer (1980), Mass spectrometric measurements of the neutral gas composition of the thermosphere and exosphere of Venus, *J. Geophys. Res.*, *85*, 7817–7828.

Rees, M. H. (1989), *Physics and Chemistry of the Upper Atmosphere*, Cambridge Univ. Press, New York.

Seiff, A., D. B. Kirk, R. E. Young, R. C. Blanchard, J. T. Findlay, G. M. Kelly, and S. C. Sommer (1980), Measurements of thermal structure and thermal contrasts in the atmosphere of Venus and related dynamical observations: Results from the four Pioneer Venus probes, *J. Geophys. Res.*, *85*, 7903–7933.

Taylor, H. A., H. C. Brinton, S. J. Bauer, R. E. Hartle, P. A. Cloutier, and R. E. Daniell (1980), Global observations of the composition and dynamics of the ionosphere of Venus: Implications for the solar wind interaction, *J. Geophys. Res.*, *85*, 7765–7777.

Theis, R. F., L. H. Brace, and H. G. Mayr (1980), Empirical models of the electron temperature and density in the Venus ionosphere, *J. Geophys. Res.*, *85*, 7787–7794.

Theis, R. F., L. H. Brace, R. C. Elphic, and H. G. Mayr (1984), New empirical models of the electron temperature and density in the Venus ionosphere with application to transterminator flow, *J. Geophys. Res.*, *89*, 1477–1488.

Tobiska, W. K. (2004), SOLAR2000 irradiances for climate change, aeronomy and space system engineering, *Adv. Space. Res.*, *34*(8), 1736–1746.

von Zahn, U., K. H. Fricke, D. M. Hunten, D. Krankowsky, K. Mauersberger, and A. O. Nier (1980), The upper atmosphere of Venus during morning conditions, *J. Geophys. Res.*, *85*, 7829–7840.

Zhang, S., S. W. Bougher, and M. J. Alexander (1996), The impact of gravity waves on the Venus thermosphere and O_2 IR nightglow, *J. Geophys. Res.*, *101*, 23,195–23,205.

J. L. Fox, Department of Physics, Wright State University, Dayton, OH 45435, USA. (jane.fox@wright.edu)

W. T. Kasprzak, NASA Goddard Space Flight Center, Code 699, Greenbelt, MD 20771, USA. (wayne.t.kasprzak@nasa.gov)